Journal of Advanced Research in Fluid Mechanics and Thermal Sciences

Journal homepage:
https://semarakilmu.com.my/journals/index.php/fluid_mechanics_thermal_sciences/index
ISSN: 2289-7879

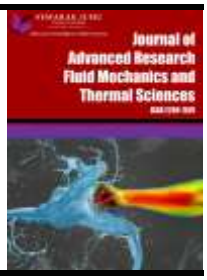

Parametric Investigation and Optimization of the Photovoltaic-Thermal Air Heater

Nguyen Van Hap[1,2], Mai Thanh Dam[3], Nguyen Hoang Khoi[4], Nguyen Minh Phu[4,*]

[1] Faculty of Mechanical Engineering, Ho Chi Minh City University of Technology (HCMUT), 268 Ly Thuong Kiet, District 10, Ho Chi Minh City, Vietnam
[2] Vietnam National University Ho Chi Minh City (VNU-HCM), Linh Trung Ward, Thu Duc City, Ho Chi Minh City, Vietnam
[3] Faculty of Mechanical Engineering and Technology, Ho Chi Minh City University of Industry and Trade (HUIT), 140 Le Trong Tan, Tan Phu District, Ho Chi Minh City, Vietnam
[4] Faculty of Heat and Refrigeration Engineering, Industrial University of Ho Chi Minh City (IUH), 12 Nguyen Van Bao, Go Vap District, Ho Chi Minh City, Vietnam

ARTICLE INFO

Article history:
Received 6 April 2024
Received in revised form 25 July 2024
Accepted 8 August 2024
Available online 30 August 2024

Keywords:
Combined heat and power (CHP); waste heat recovery; PV/T; lumped parameter model; metaheuristic approach

ABSTRACT

Co-generation of heat and electricity from solar cells is an energy efficient option because the photovoltaic (PV) efficiency is less than twenty percent, the rest goes to heat. In this paper, the heat emitted from the PV panel is used to produce hot air which is useful heat and to reduce the PV cell temperature thereby increasing the system performance. Independent parameters include air mass flow rate ($\dot{m}_{air}$), air channel height (H), PV panel aspect ratio (R_a), and environmental parameters (temperature, wind velocity, solar intensity) to investigate their influence on power and heat generation, and performances. The mathematical description of the system is formed using a lumped parameter model. The analytical results show that the overall performance is maximized at certain design parameters. This phenomenon is due to the trade-off between power generation, heat output, and fan power with a design specification. Optimizing the overall efficiency using a genetic algorithm (GA), which is a metaheuristic based on the principles of natural selection and categorized as part of the broader group of evolutionary algorithms, yields the maximum value of 98.76% at the optimal parameters $\dot{m}_{air}$= 0.3032 kg/s, H = 27.37 mm, and R_a = 1.809.

1. Introduction

Photovoltaics (PV) is an advanced technological device that uses solar energy to convert into electricity. It is a simple and compact generator, much more flexible than the vapor power cycle. Today PV is installed everywhere to take advantage of the huge solar energy resources and reduce dependence on fossil fuels. It can be installed on rooftops, lakes, deserts, on the roofs of mobile devices (cars, ships, airplanes) or outer space. The forecast installed capacity by 2040 will be more than 600 GW, double that of the 2020s [1]. Although solar power technology continues to develop, the efficiency of solar cells is still below 20%. In other words, most of the solar radiation is absorbed

* *Corresponding author.*
E-mail address: nguyenminhphu@iuh.edu.vn

https://doi.org/10.37934/arfmts.120.2.6781

by the panel and converted into heat energy [2]. Power generation efficiency will decrease if the panels are not cooled properly [3]. Therefore, the integration of solar cells that produce electricity and heat simultaneously (PV/T) is a reasonable combination to increase system performance [4,5]. The temperature of the PV system dropped by 6.6°C, leading to a 4.0% increase in power generation efficiency [6]. This heat can be used in hot air drying, hot water production, distillation, or the evaporator of a heat pump.

Research on PV/T system for drying, Tiwari and Tiwari [7] employed a PV-integrated greenhouse dryer in unload conditions. The largest thermal energy obtained is 3.26 kWh for a PV area of 1.2 m^2. Gupta *et al.,* [8] employed hot air from PV to dry star fruit in natural and forced convection modes. Their systems achieved the highest PV efficiency and overall efficiency of 13.58% and 69.27%, respectively. Research on the environmental impact of a PV/T system, Tripathi *et al.,* [9] analyzed the carbon credit of the PV/T concentrating collector. They concluded that 25% PV coverage provides maximum carbon reduction. Research on heating a liquid, Khani *et al.,* [10] used genetic algorithm (GA) to optimize the thermal and electrical performance of the PV/T collector. Waste heat from PV is used to produce hot water. The mathematical model includes two-dimensional unsteady energy equations. Optimal results indicate a 25% increase in efficiency compared to a stand-alone PV. Rejeb *et al.,* [11] utilized heat from PV cells to heat a nanofluid. They concluded that solar irradiance and flow rate dramatically affect the performance system. Guo *et al.,* [12] produced hot water from PV thermal dissipation. This hot water heats the air to regenerate the desiccant wheel. Heat from PV can meet full demand for temperate climates and high solar radiation. Rosli *et al.,* [13] connected PV/T collector with a phase change material (PCM) in a research of numerical simulation. They proved that the overall efficiency was up to 90.82%. Recently, Choi and Choi [14] comprehensively evaluated a PV/T system to supply thermal energy to a heat pump that produces hot water. Performance of the proposed system is improved up to 13.28% compared to traditional heat pumps. Research on design parameters and cooling PV, Hoang *et al.,* [15] compared four PV/T configurations via evaluation of first and second laws. They confirmed that the highest thermal efficiency was 54.185% and the greatest electrical efficiency was 13.67%. These peak efficiencies are due to the configuration with air gap which acts as a heat trap reducing heat loss. More recently, Soliman [16] offered five PV cooling models with air or water. Energy and exergy analysis were performed by solving the system of linear equations in MATLAB. The results have been reported that the heat transfer fluid of water is more efficient at 90% efficiency compared to 34% if cooled by air.

The above literature review reveals that investigating the influence of multi-parameters including design parameters and weather parameters on electrical-thermohydraulic performance of an air-cooled PV/T collector is rare to find. The investigation is important because PV cell temperature has opposite effects on electrical power, useful heat, and fan power. Therefore, optimal parameters can be found to maximize system performance. In this study the effects of three design parameters and three weather parameters are evaluated and the optimal parameters are sought. A mathematical model for the PV/T collector is established to investigate the parameters and present the results of the optimization.

2. Mathematical Formulation

Simultaneous generations of power and thermal energy are presented in Figure 1. Photovoltaic (PV) panel is placed above to capture solar energy. Below the panel is an air flow to receive heat from the PV panel due to thermal generation during the process of converting solar energy into electricity. The lowest is the back surface with insulation to reduce heat loss. The energy balance equations for the five components (glass, PV cell, tedlar, airflow, and back surface) are written below [17,18].

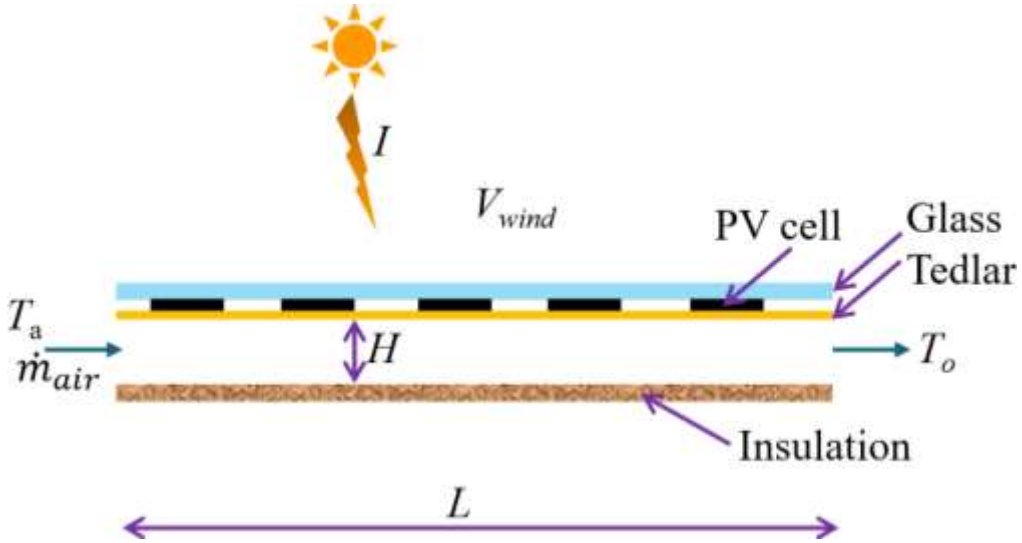

Fig. 1. Schematic diagram of the photovoltaic-thermal air heater

The glass absorbs solar energy in balance with heat transferred by convection to the wind above, thermal radiation to the sky, and heat conduction from the glass to the PV cell

$$\alpha_g \cdot I = h_{wind} \cdot \left(T_g - T_a\right) + h_{r,g,s} \cdot \left(T_g - T_s + 273\right) + U_{g,c} \cdot \left(T_g - T_c\right) \tag{1}$$

The heat passing through the glass is absorbed by the PV cell and converted into heat energy in balance with heat conduction from the cell to the glass and to the tedlar

$$\tau_g \cdot \alpha_c \cdot I \cdot \zeta \cdot \left(1 - \eta_{el}\right) = U_{g,c} \cdot \left(T_c - T_g\right) + U_{c,ted} \cdot \left(T_c - T_{ted}\right) \tag{2}$$

The heat absorbed by the tedlar is balanced by heat conduction between the cell and the tedlar, and convection heat transfer with the air flow

$$\tau_g \cdot \alpha_{ted} \cdot I \cdot \left(1 - \zeta\right) = U_{c,ted} \cdot \left(T_{ted} - T_c\right) + U_{ted,air} \cdot \left(T_{ted} - T_{air}\right) \tag{3}$$

The useful thermal energy received by the air flow through the PV panel is balanced with the heat transferred by convection to the tedlar and back surface

$$\dot{Q} = \dot{m}_{air} \cdot c_{p,air} \cdot \left(T_o - T_a\right) = L \cdot W \cdot h_{air} \cdot \left(T_{ted} - T_{air} + T_b - T_{air}\right) \tag{4}$$

The back surface receives radiant thermal energy from the tedlar in balance with convective heat transfer with the air current and heat loss through the insulation layer

$$h_{r,ted,b} \cdot \left(T_{ted} - T_b\right) = h_{air} \cdot \left(T_b - T_{air}\right) + h_b \cdot \left(T_b - T_a\right) \tag{5}$$

In the above equations, the average air temperature (T_{air}) is the average of the air temperatures entering and leaving the PV panel

$$T_{air} = 0.5 \cdot \left(T_a + T_o\right) \tag{6}$$

The sky temperature (T_s in Kelvin) is calculated from the ambient temperature (T_a) as follows [19]

$$T_s = 0.0552 \cdot \left(T_a + 273\right)^{1.5} \tag{7}$$

The convective heat transfer coefficient of the wind is calculated from the McAdam's equation [20]

$$h_{wind} = 5.7 + 3.8 \cdot V_{wind} \tag{8}$$

Radiant heat transfer coefficients

$$h_{r,g,s} = \sigma \cdot \varepsilon_g \cdot \left(\left(T_g + 273\right)^2 + T_s^{\,2}\right) \cdot \left(T_g + 273 + T_s\right) \tag{9}$$

$$h_{r,ted,b} = \sigma \cdot \left(\left(T_{ted} + 273\right)^2 + \left(T_b + 273\right)^2\right) \cdot \frac{T_{ted} + 273 + T_b + 273}{1/\varepsilon_{ted} + 1/\varepsilon_b - 1} \tag{10}$$

Combined heat transfer coefficients

$$U_{g,c} = \left(\frac{\delta_g}{k_g} + \frac{\delta_c}{2 \cdot k_c}\right)^{-1} \tag{11}$$

$$U_{c,ted} = \left(\frac{\delta_{ted}}{2 \cdot k_{ted}} + \frac{\delta_c}{2 \cdot k_c}\right)^{-1} \tag{12}$$

$$U_{ted,air} = \left(\frac{\delta_{ted}}{2 \cdot k_{ted}} + 1/h_{air}\right)^{-1} \tag{13}$$

Heat transfer coefficient due to conduction through the insulation at the back surface

$$h_b = k_i / \delta_i \tag{14}$$

The convective heat transfer coefficient of the air with the tedlar and with the back surface (h_{air}) is calculated from the Dittus-Boelter equation as follows [20]

$$Nu = 0.021 \cdot Re^{0.8} \cdot Pr^{0.4} \tag{15}$$

$$h_{air} = k_{air} \cdot Nu / D_h \tag{16}$$

where

- hydraulic diameter: $D_h = 4 \cdot W \cdot \frac{H}{2 \cdot \left(W + H\right)}$ (17)

- Reynolds number: $Re = V \cdot D_h \cdot \rho_{air} / \mu_{air}$ (18)

To calculate the pressure loss through the smooth channel, the Blasius friction coefficient equation is used as follows

$$f = 0.3164 \cdot Re^{-0.25} \tag{19}$$

From there, the air pressure loss through the PV panel is calculated as follows [21]

$$\Delta P = f \cdot \rho_{air} \cdot L \cdot \frac{V^2}{2 \cdot D_h} \tag{20}$$

Fan power

$$\dot{W}_{fan} = \dot{m}_{air} \cdot \frac{\Delta P}{\rho_{air} \cdot \eta_{fan}} \tag{21}$$

where

Air mass flow rate: $\dot{m}_{air} = V \cdot W \cdot H \cdot \rho_{air}$ (22)

Fan efficiency: $\eta_{fan} = 0.5$

Net power generation

$$\dot{W}_{el} = I \cdot L \cdot W \cdot \eta_{el} - \dot{W}_{fan} \tag{23}$$

where η_{el} is the efficiency of the PV which depends on the cell temperature and standard electrical efficiency (η_{stc})

$$\eta_{el} = \eta_{stc} \cdot \left(1 + \gamma \cdot \left(T_c - 25\right)\right) \tag{24}$$

Thermal efficiency

$$\eta_{th} = \frac{\dot{Q}}{I \cdot L \cdot W} \tag{25}$$

Electrical efficiency

$$\eta_{el,net} = \frac{\dot{W}_{el}}{I \cdot L \cdot W} \tag{26}$$

Overall efficiency

$$\eta_{overall} = \eta_{th} + \eta_{el,net} / 0.38 \tag{27}$$

Table 1 and Table 2 present the input parameters and the range of independent parameters to investigate $\dot{Q}$, $\dot{W}_{el}$, η_{th}, $\eta_{el,net}$, and $\eta_{overall}$ corresponding to 1 m^2 PV panel area. The six independent factors included weather conditions (solar radiation, wind, ambient temperature), geometries of PV/T (aspect ratio, air channel height), and operating condition (air flow rate). They are the essential factors affecting the performance of a photovoltaic-thermal air heater. A simulation program is written in EES software (F-chart software). Thermophysical parameters of the air (density ρ_{air}, specific heat $c_{p,air}$, viscosity μ_{air}, conductivity k_{air}, Prandtl number Pr) were taken at the ambient temperature T_a. The software EES is versatile software for solving equations that has the capability to numerically solve numerous interconnected non-linear algebraic equations. By counting the number of variables and number of equations, EES may give a solution if the numbers are identical.

Table 1
Parameters of the modelling [14,17,22]

Parameter	Value
Absorptivity of glass	$\alpha_g = 0.06\ [-]$
Emissivity of glass	$\varepsilon_g = 0.93\ [-]$
Thickness of glass	$\delta_g = 0.003\ [\mathrm{m}]$
Conductivity of glass	$k_g = 1\ [\mathrm{W/m \cdot K}]$
Thickness of PV cell	$\delta_c = 0.0003\ [\mathrm{m}]$
Conductivity of PV cell	$k_c = 0.036\ [\mathrm{W/m \cdot K}]$
Thickness of tedlar	$\delta_{ted} = 0.0005\ [\mathrm{m}]$
Conductivity of tedlar	$k_{ted} = 0.033\ [\mathrm{W/m \cdot K}]$
Transmissivity of glass	$\tau_g = 0.9\ [-]$
Absorptivity of PV cell	$\alpha_c = 0.85\ [-]$
Coverage factor of PV cell	$\zeta = 0.9288\ [-]$
Standard electrical efficiency	$\eta_{stc} = 0.1737\ [-]$
Temperature coefficient	$\gamma = -0.0041\ [1/\mathrm{C}^{-1}]$
Thickness of PV cell	$\alpha_{ted} = 0.8\ [-]$
PV area	$L \cdot W = 1m^2$
Thickness of insulation	$\delta_i = 0.05\ [\mathrm{m}]$
Conductivity of insulation	$k_i = 0.025\ [\mathrm{W/m \cdot K}]$
Emissivity of tedlar	$\varepsilon_{ted} = 0.9$
Emissivity of back surface	$\varepsilon_b = 0.94\ [-]$

Table 2
Range of the independent parameters

No.	Parameter	Range	Base case
1	Solar radiation	$I = 100 - 1000\ \mathrm{W/m^2}$	1000 W/m^2
2	Wind velocity	$V_{wind} = 0 - 5\ \mathrm{m/s}$	2 m/s
3	Ambient temperature	$T_a = 25 - 40\ ^\circ C$	30 °C
4	Aspect ratio	$R_a = 1 - 4$	1
5	Air channel height	$H = 0.01 - 0.04\ \mathrm{m}$	0.02 m
6	Air mass flow rate	$\dot{m}_{air} = 0.01 - 0.35\ \mathrm{kg/s}$	0.075 kg/s

First, the numerical results are compared with published data to ensure reliability. Figure 2 shows a comparison of the air temperature leaving the PV panel (T_o) and the cell temperature (T_c) with air mass flow rate. The input parameters in the two approaches are the same. In the previous publication, the back surface of the PV-thermal air heater is equipped with triangular blocks to enhance heat transfer [14]. Therefore, the Nusselt number equation is also shown in the figure. The results in Figure 2 demonstrate that there is an absolute coincidence of cell temperature. For temperature T_o, the results in this study are slightly higher than published data. This deviation is because the previous study considered the variation of air temperature along the direction of motion (one-dimensional). Meanwhile, this study used a lumped parameter model (zero-dimensional).

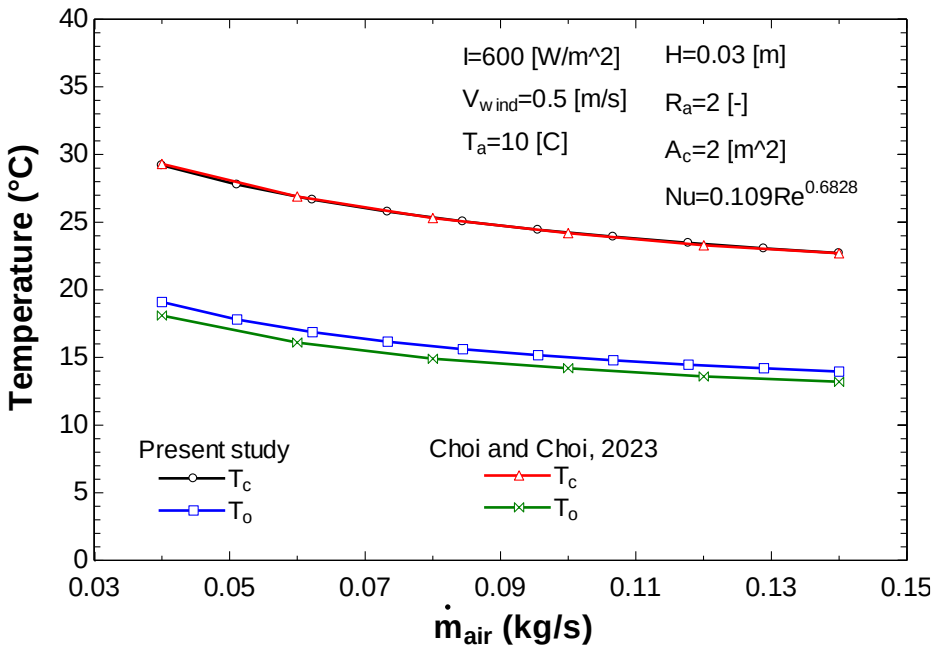

Fig. 2. Verification of the current work with the published data [14]

3. Results and Discussion

Investigation of the influence of six parameters on the performance of the PV/T system is presented in this section. When an independent parameter changes, the remaining five parameters are kept constant as the base case in Table 2. The effect of air mass flow rate is presented in Figure 3 and Figure 4. As the flow rate increases, the convective heat transfer coefficient of the air (h_{air}) increases thereby increasing the useful heat as shown in Figure 3. The heat transfer rate increases from 136 W to 604 W when the flow rate increases from 0.01 kg/s to 0.35 kg/s. For electrical power,

increased flow rate reduces the cell temperature (T_c) thus increasing power generation. However, fan power increases sharply with the flow rate (approximate third power). Therefore, net power generation reaches its maximum at an air flow of about 0.075 kg/s. The power generation capacity is much smaller than the thermal capacity due to the PV efficiency being below 20%. Therefore, simultaneously thermal and power generation is a desirable solution. The trends of electrical efficiency and thermal efficiency are like those of power generation and useful heat as shown in Figure 4. At high flow rate, thermal efficiency increases, and electrical efficiency decreases so the overall efficiency reaches maximum of 90% at flow rate of 0.275 kg/s.

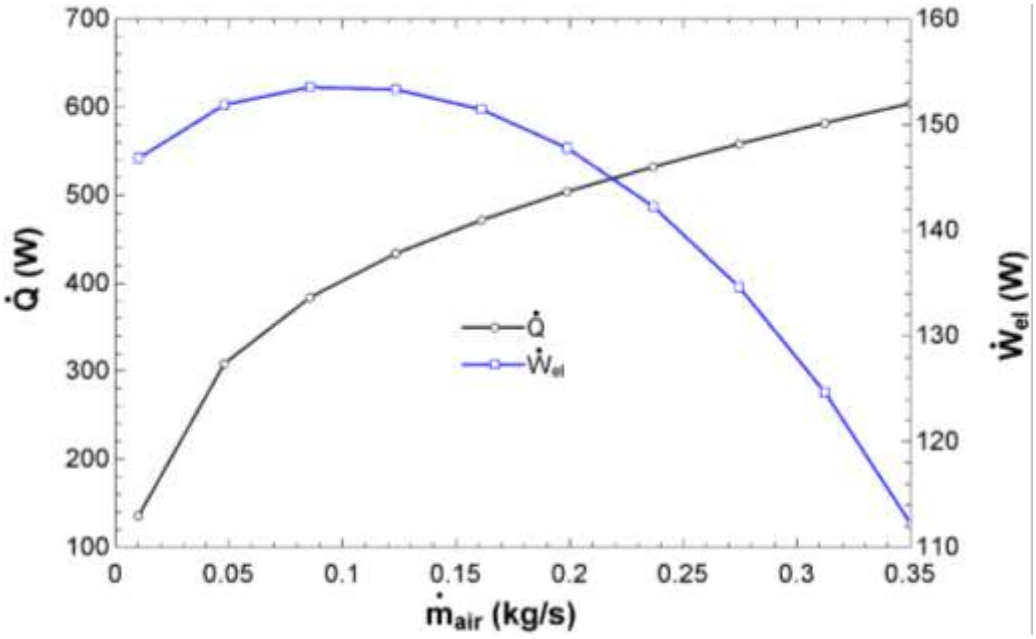

Fig. 3. Power generation and useful heat with air mass flow rates

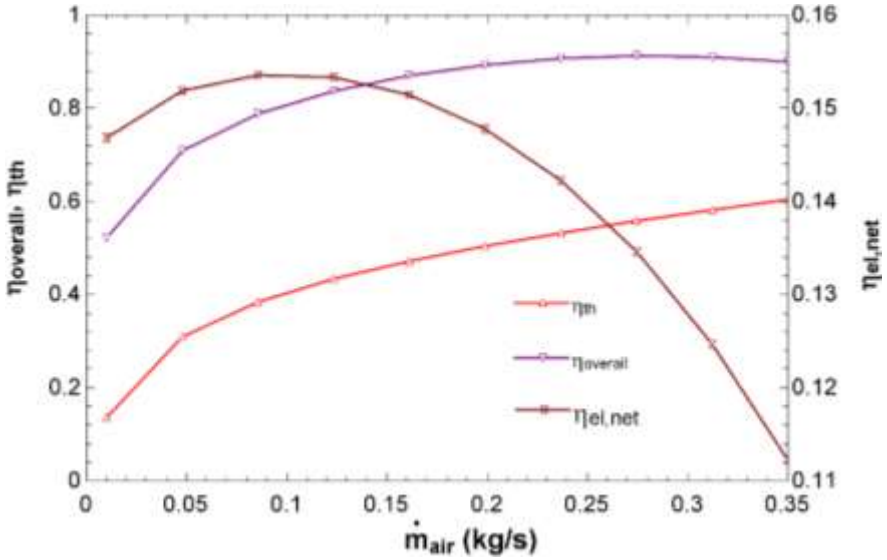

Fig. 4. Efficiencies with air mass flow rates

The effect of radiation intensity is shown in Figure 5 and Figure 6. It is clear that as radiation increases, the thermal and electrical powers increase sharply as shown in Figure 5. The slope of the power generation is less than that of heat transfer rate, $\dot{W}_{el}$ =3.2 + 0.15I vs. $\dot{Q}$ =-33.8 + 0.4I. This is because increased radiation increases cell temperature thereby reducing PV efficiency (η_{el}). The

trade-off between increasing radiation and decreasing efficiency causes the power generation efficiency to peak at I = 200 W/m^2. However, the power generation efficiency insignificantly changes with radiation. When the radiation changes from 100 to 1000 W/m^2, the power generation efficiency changes from 15.3% to 16.4%. From the trends of thermal efficiency and power generation efficiency, the overall efficiency is almost unchanged when the radiation is greater than 700 W/m^2.

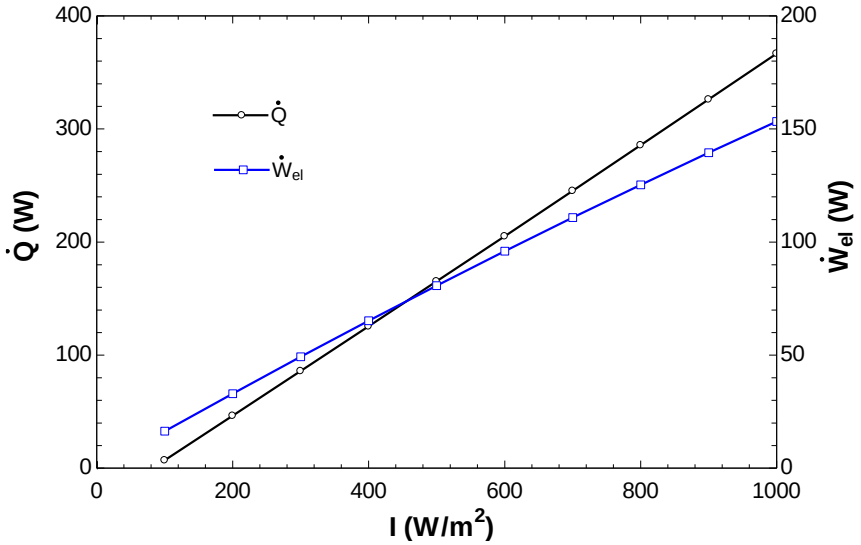

Fig. 5. Power generation and useful heat under various solar intensities

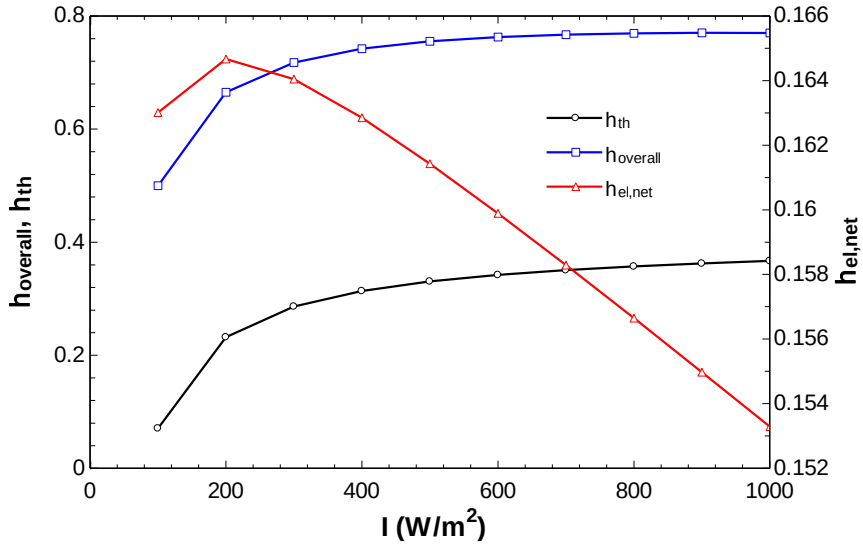

Fig. 6. Efficiencies under various solar intensities

The impact of the aspect ratio of the PV panel is presented in Figure 7 and Figure 8. When R_a is greater than unity and increases, i.e. the PV length L is greater than the PV width W, the air speed is greater because W decreases. In addition, the air travels on the longer heat exchange surface, so the heat exchange is greater. High air velocity reduces cell temperature thereby increasing PV performance. However, increasing V and L increases the fan power, so the net power generation reaches its maximum at R_a = 1.7. The influence of R_a on heat output is much greater than on electricity generation. Therefore, the overall efficiency increases with the thermal efficiency as shown in Figure 8. The heat transfer rate and the overall efficiency increase from 367 W to 445 W and 77% to 84.5%, respectively, when the aspect ratio increases from 1 to 4.

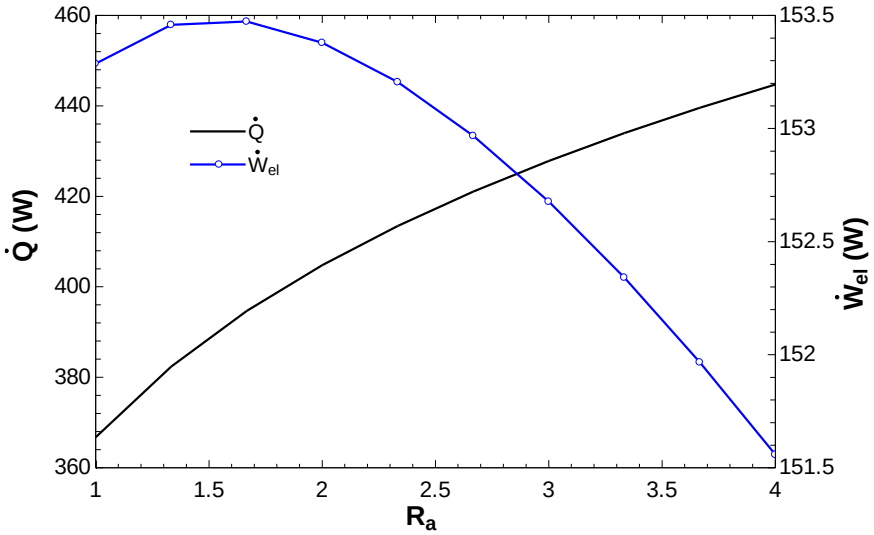

Fig. 7. Effect of aspect ratio on power generation and useful heat

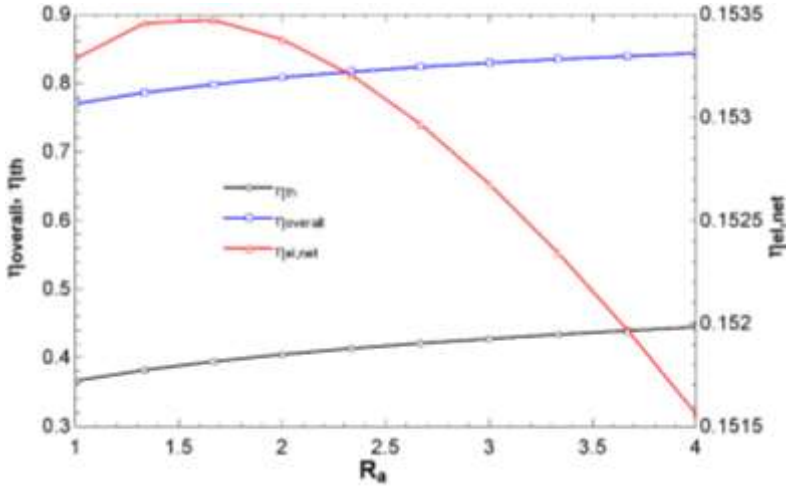

Fig. 8. Effect of aspect ratio on efficiencies

Variation of the operating parameters with air channel height is presented in Figure 9 and Figure 10. As height increases, air velocity decreases, thus reducing forced convective heat transfer. Therefore, the heat transfer rate decreases sharply with the increase of H. The heat transfer rate decreases from 465 W to 275 W when the channel height increases from 0.01 m to 0.05 m. Increasing H reduces fan power and increases cell temperature. These two opposing trends cause the power generation to reach its maximum at H of about 17.5 mm. The power generation varies little with H, so the overall efficiency is dominated by thermal efficiency. So, when H increases, the overall efficiency decreases.

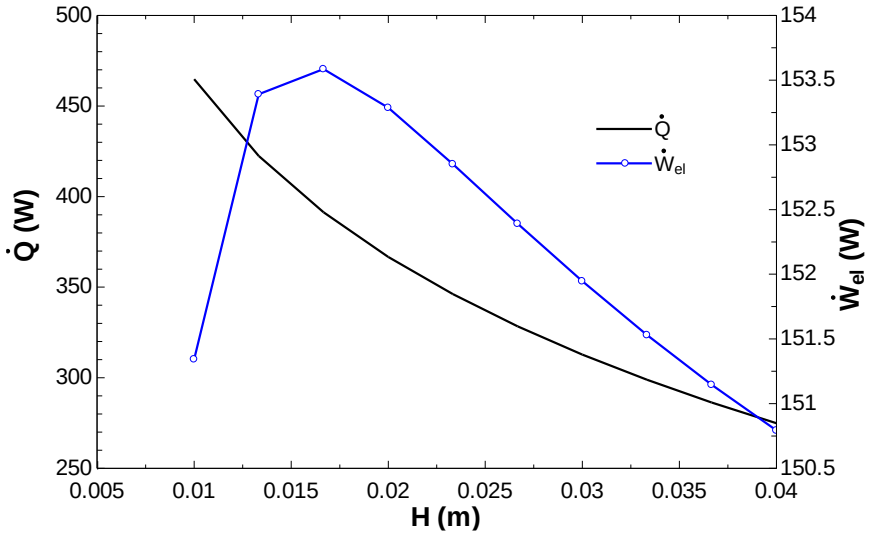

Fig. 9. Power generation and useful heat for different air channel heights

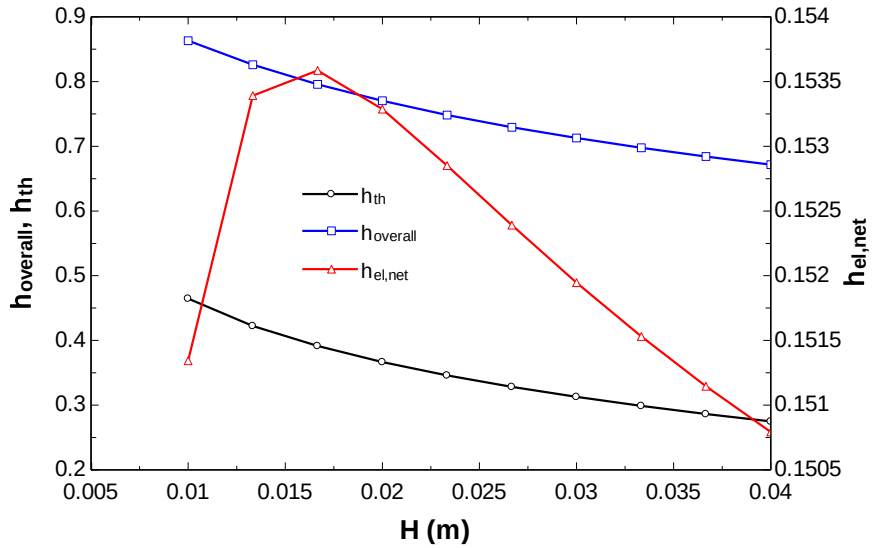

Fig. 10. Efficiencies for different air channel heights

The impact of the surrounding environment is shown in Figure 11 to Figure 14. The effect of the upper wind speed on the PV panel is shown in Figure 11 and Figure 12. As the wind speed increases leading to increase in heat loss and decrease in cell temperature, so the useful heat is reduced, and the power generation is increased. The change in useful heat is more significant, so the overall efficiency follows the trend of thermal efficiency. That is, increasing wind speed reduces overall efficiency. The effect of environmental temperature is presented in Figure 13 and Figure 14. When the ambient temperature increases, the radiant heat transfer coefficient and forced convection heat transfer coefficient of the air increase, thereby increasing the thermal energy and thermal performance. However, increased ambient temperature increases the PV temperature, thereby reducing power generation. The increase in heat output and decrease in power generation result in an overall efficiency that remains nearly constant with ambient temperature.

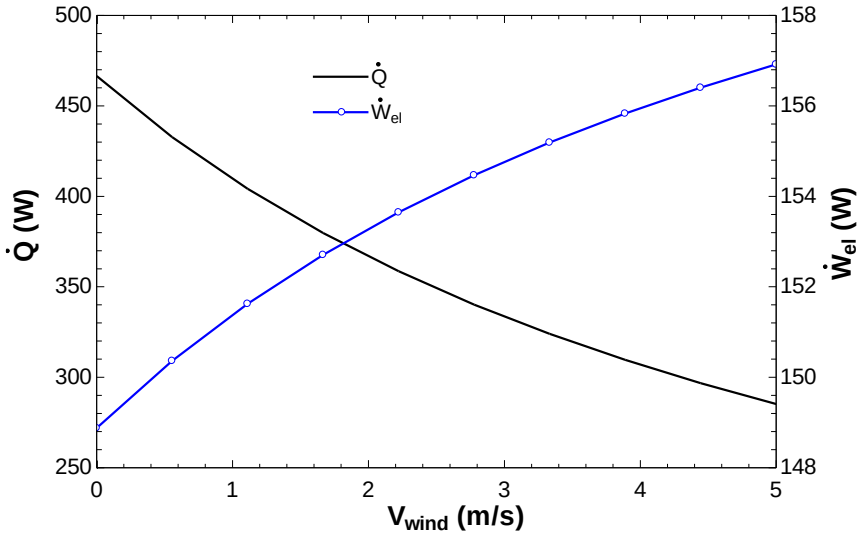

Fig. 11. Variation of power generation and useful heat as a function of wind velocity

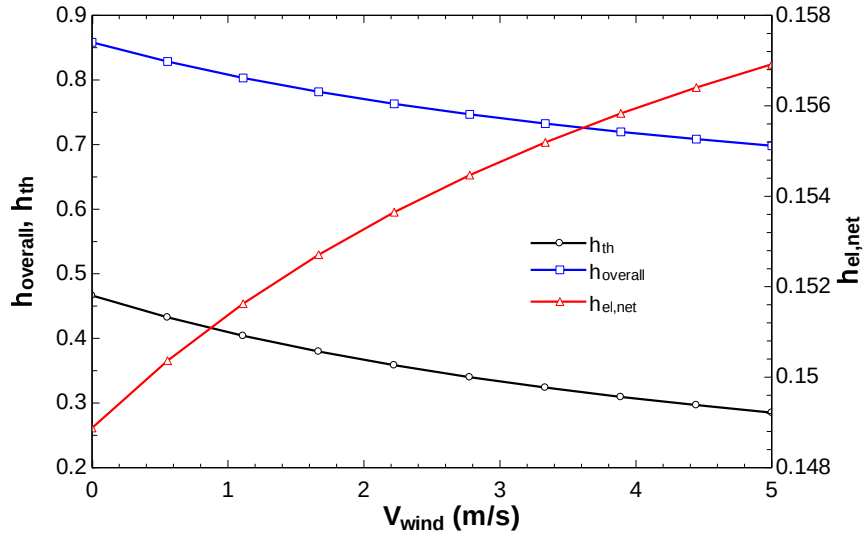

Fig. 12. Variation of efficiencies as a function of wind velocity

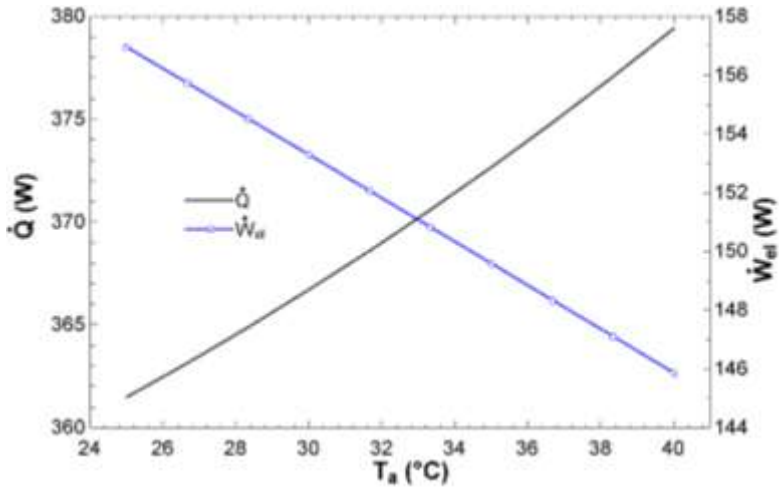

Fig. 13. Power generation and useful heat with respect to ambient temperature

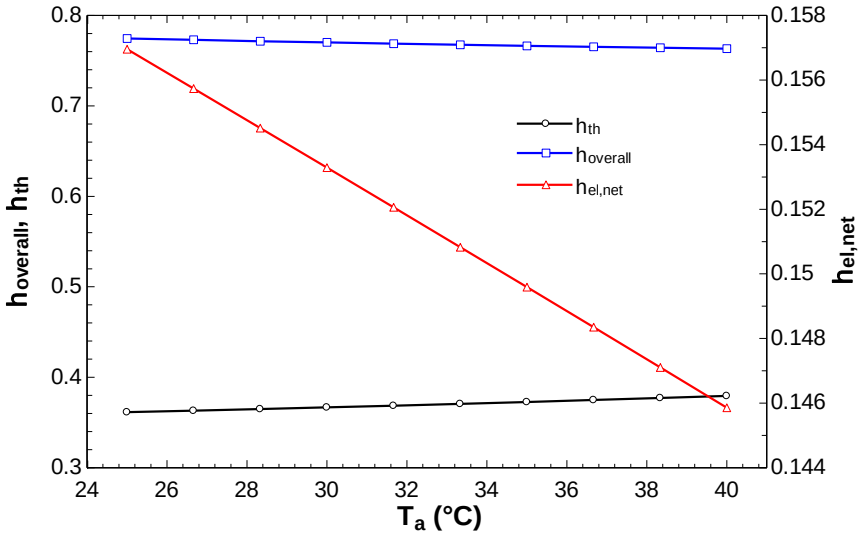

Fig. 14. Efficiencies with respect to ambient temperature

Examination of the six parameters above indicates that entire performance can be maximized at the optimal values of air flow, aspect ratio, and air channel height. In this study, genetic algorithm (GA) in EES software was used to find the maximum overall performance according to six independent parameters with the range given in Table 2. Table 3 presents the setting values of the parameters used in the optimization. As shown in Table 4, the overall efficiency of the base case of 77.01% can be further improved. Optimal results were achieved after generation number of 64. The optimal parameters are presented in Table 4 corresponding to an overall efficiency of 98.76%. This performance is much greater than the performance of the base case. The optimal design parameters obtained include R_a = 1.809, H = 27.27mm, and $\dot{m}_{air}$ = 0.3032 kg/s corresponding to 1 m^2 PV panel area.

Table 3
Parameters of the optimization genetic algorithm

Parameter	Range	Setting value	Remark
Number of individuals	16 to 128	16	The initial choice is made randomly within the range defined by the independent variables' bounds.
Number of generations	16 to 2048	580	When the number of generations reaches the value, the algorithm comes to a stop.
Maximum mutation rate	0.0875 to 0.7	0.175	The algorithm will aggressively search for an optimum in distant locations when larger values are used. When smaller values are used, the search will be focused more around the current optimum.

Table 4
Optimization using GA in EES

No.	Parameter	Base case	Optimum value
1	Solar radiation	1000 W/m^2	1000 W/m^2
2	Wind velocity	2 m/s	0.1339 m/s
3	Ambient temperature	30 °C	32.25 °C
4	Aspect ratio	1	1.809
5	Air channel height	0.02 m	0.02737 m
6	Air mass flow rate	0.075 kg/s	0.3032 kg/s
7	Overall efficiency	0.7701	0.9876

4. Conclusions

In this paper, the mathematical formulation for the PV/T system is established and solved according to the lumped parameter model including five equations for the five components of the system. The system of equations is solved in the EES environment, and the results are compared with published data. Thermal and electrical performance was investigated with three design parameters and three environmental parameters. Parametric study results show that air flow rate, aspect ratio, and channel height have optimal values to achieve the highest overall efficiency. Optimizing the efficiency using genetic algorithm exhibits the efficiency of 98.76% with optimal design parameters consisting of flow rate of 0.3032 kg/s, channel height of 27.37 mm, and aspect ratio of 1.809. The output data showed that the GA model suggested was suitable to predict PV/T variables. Appropriate sizes of individual components for a given heat and power capacity or climatic conditions may be used based on the current model and corresponding PV/T simulation programs. The entire system and its real-time behavior should be taken into account in further research.

Acknowledgement

The author Nguyen Van Hap acknowledges Ho Chi Minh City University of Technology (HCMUT), VNU-HCM for supporting this study.

References

[1] Diwania, Sourav, Sanjay Agrawal, Anwar S. Siddiqui, and Sonveer Singh. "Photovoltaic-thermal (PV/T) technology: a comprehensive review on applications and its advancement." *International Journal of Energy and Environmental Engineering* 11 (2020): 33-54. https://doi.org/10.1007/s40095-019-00327-y

[2] Joshi, Sandeep S., and Ashwinkumar S. Dhoble. "Photovoltaic-Thermal systems (PVT): Technology review and future trends." *Renewable and Sustainable Energy Reviews* 92 (2018): 848-882. https://doi.org/10.1016/j.rser.2018.04.067

[3] Hồ, Huy Đăng, and Viết Văn Hoàng. "Thermal analysis of water distillation system using pv/t collector combined single basin still." *VNUHCM Journal of Engineering and Technology* 5, no. 4 (2022): 1661-1678.

[4] Sopian, Kamaruzzaman, K. S. Yigit, H. T. Liu, S. Kakac, and T. N. Veziroglu. "Performance analysis of photovoltaic thermal air heaters." *Energy Conversion and Management* 37, no. 11 (1996): 1657-1670. https://doi.org/10.1016/0196-8904(96)00010-6

[5] Abdullah, Amira Lateef, Suhaimi Misha, Noreffendy Tamaldin, Mohd Afzanizam Mohd Rosli, and Fadhil Abdulameer Sachit. "Technology progress on photovoltaic thermal (PVT) systems with flat-plate water collector designs: a review." *Journal of Advanced Research in Fluid Mechanics and Thermal Sciences* 59, no. 1 (2019): 107-141.

[6] Huang, Lin, Zihao Song, Qichang Dong, Ye Song, Xiaoqing Zhao, Jiacheng Qi, and Long Shi. "Surface temperature and power generation efficiency of PV arrays with various row spacings: A full-scale outdoor experimental study." *Applied Energy* 367 (2024): 123362. https://doi.org/10.1016/j.apenergy.2024.123362

[7] Tiwari, Sumit, and G. N. Tiwari. "Thermal analysis of photovoltaic-thermal (PVT) single slope roof integrated greenhouse solar dryer." *Solar Energy* 138 (2016): 128-136. https://doi.org/10.1016/j.solener.2016.09.014

[8] Gupta, Ankur, Biplab Das, Agnimitra Biswas, and Jayanta Deb Mondol. "Sustainability and 4E analysis of novel solar photovoltaic-thermal solar dryer under forced and natural convection drying." *Renewable Energy* 188 (2022): 1008-1021. https://doi.org/10.1016/j.renene.2022.02.090

[9] Tripathi, Rohit, G. N. Tiwari, and V. K. Dwivedi. "Overall energy, exergy and carbon credit analysis of N partially covered photovoltaic thermal (PVT) concentrating collector connected in series." *Solar Energy* 136 (2016): 260-267. https://doi.org/10.1016/j.solener.2016.07.002

[10] Khani, M. S., M. Baneshi, and M. Eslami. "Bi-objective optimization of photovoltaic-thermal (PV/T) solar collectors according to various weather conditions using genetic algorithm: A numerical modeling." *Energy* 189 (2019): 116223. https://doi.org/10.1016/j.energy.2019.116223

[11] Rejeb, Oussama, Chaouki Ghenai, Mohamed Hedi Jomaa, and Maamar Bettayeb. "Statistical study of a solar nanofluid photovoltaic thermal collector performance using response surface methodology." *Case Studies in Thermal Engineering* 21 (2020): 100721. https://doi.org/10.1016/j.csite.2020.100721

[12] Guo, Jinyi, Jose I. Bilbao, and Alistair B. Sproul. "Parametric number of transfer unit analysis of a photovoltaic thermal coupled desiccant dehumidifier." *Energy Conversion and Management* 255 (2022): 115339. https://doi.org/10.1016/j.enconman.2022.115339
[13] Rosli, Mohd Afzanizam Mohd, Siti Nur Dini Noordin Saleem, Nortazi Sanusi, Nurfarhana Salimen, Safarudin Gazali Herawan, and Qaharuddin Abdullah. "Performance Optimization of a Simulation Study on Phase Change Material for Photovoltaic Thermal." *CFD Letters* 14, no. 9 (2022): 32-51. https://doi.org/10.37934/cfdl.14.9.3251
[14] Choi, Hwi-Ung, and Kwang-Hwan Choi. "Numerical study on the performance of a solar-assisted heat pump coupled with a photovoltaic-thermal air heater." *Energy* 285 (2023): 129480. https://doi.org/10.1016/j.energy.2023.129480
[15] Hoang, Viet Van, Hiep Chi Le, and Bao The Nguyen. "Energy, Exergy Efficiency and Thermal-Electrical Production Assessment for an Active Water Heating System Using Four PV/T Module Models." *Energies* 15, no. 24 (2022): 9634. https://doi.org/10.3390/en15249634
[16] Soliman, Ahmed Mohamed. "A numerical investigation of PVT system performance with various cooling configurations." *Energies* 16, no. 7 (2023): 3052. https://doi.org/10.3390/en16073052
[17] Choi, Hwi-Ung, and Kwang-Hwan Choi. "Electrical and Thermal Performances of a Single-Pass Double-Flow Photovoltaic-Thermal Collector Coupled with Nonuniform Cross-Section Rib." *International Journal of Energy Research* 2023, no. 1 (2023): 4744558. https://doi.org/10.1155/2023/4744558
[18] Hai, Doan Thi Hong, and Nguyen Minh Phu. "A critical review of all mathematical models developed for solar air heater analysis." *Journal of Advanced Research in Fluid Mechanics and Thermal Sciences* 105, no. 1 (2023): 1-14. https://doi.org/10.37934/arfmts.105.1.114
[19] Phu, Nguyen Minh, Ngo Thien Tu, and Nguyen Van Hap. "Thermohydraulic performance and entropy generation of a triple-pass solar air heater with three inlets." *Energies* 14, no. 19 (2021): 6399. https://doi.org/10.3390/en14196399
[20] Nhut, Le Minh, Ha Nguyen Minh, and Luan Nguyen Thanh. "The Effective and Exergy Efficiency of Multi-Pass Solar Air Collector with Longitudinal Fins: Analysis and Optimization." *Journal of Advanced Research in Fluid Mechanics and Thermal Sciences* 102, no. 2 (2023): 42-65. https://doi.org/10.37934/arfmts.102.2.4265
[21] Phu, Nguyen Minh, and Nguyen Thanh Luan. "A review of energy and exergy analyses of a roughened solar air heater." *Journal of Advanced Research in Fluid Mechanics and Thermal Sciences* 77, no. 2 (2021): 160-175. https://doi.org/10.37934/arfmts.77.2.160175
[22] Luan, Nguyen Thanh, and Nguyen Minh Phu. "First and Second Law Evaluation of Multipass Flat-Plate Solar Air Collector and Optimization Using Preference Selection Index Method." *Mathematical Problems in Engineering* 2021, no. 1 (2021): 5563882. https://doi.org/10.1155/2021/5563882